



Elastic moduli of multiblock copolymers in the lamellar phase

R. B. Thompson, K. O. Rasmussen, and T. Lookman

Citation: *The Journal of Chemical Physics* **120**, 3990 (2004); doi: 10.1063/1.1643899

View online: <http://dx.doi.org/10.1063/1.1643899>

View Table of Contents: <http://scitation.aip.org/content/aip/journal/jcp/120/8?ver=pdfcov>

Published by the [AIP Publishing](#)

Articles you may be interested in

[Perpendicular lamellar-in-lamellar and other planar morphologies in A-b-\(B-b-A\)₂-b-C and \(B-b-A\)₂-b-C ternary multiblock copolymer melts](#)

J. Chem. Phys. **139**, 084906 (2013); 10.1063/1.4818872

[Nonmonotonic incommensurability effects in lamellar-in-lamellar self-assembled multiblock copolymers](#)

J. Chem. Phys. **130**, 204901 (2009); 10.1063/1.3138903

[Chain bridging in a model of semicrystalline multiblock copolymers](#)

J. Chem. Phys. **130**, 054904 (2009); 10.1063/1.3072339

[Viscoelastic behavior of cubic phases in block copolymer melts](#)

J. Rheol. **43**, 167 (1999); 10.1122/1.550981

[Elastic properties of homopolymer-homopolymer interfaces containing diblock copolymers](#)

J. Chem. Phys. **108**, 4662 (1998); 10.1063/1.475877

NEW Special Topic Sections

NOW ONLINE
Lithium Niobate Properties and Applications:
Reviews of Emerging Trends

AIP Applied Physics Reviews

The advertisement features a blue background with a molecular structure of spheres and rods. On the left is a thumbnail of an Applied Physics Reviews journal cover showing a 3D lattice structure and a graph. The text is in white and orange.

Elastic moduli of multiblock copolymers in the lamellar phase

R. B. Thompson,^{a)} K. Ø. Rasmussen,^{b)} and T. Lookman

Theoretical Division, Los Alamos National Laboratory, Los Alamos, New Mexico 87545

(Received 26 August 2003; accepted 1 December 2003)

We study the linear elastic response of multiblock copolymer melts in the lamellar phase, where the molecules are composed of tethered symmetric AB diblock copolymers. We use a self-consistent field theory method, and introduce a real space approach to calculate the tensile and shear moduli as a function of block number. The former is found to be in qualitative agreement with experiment. We find that the increase in bridging fraction with block number, that follows the increase in modulus, is *not* responsible for the increase in modulus. It is demonstrated that the change in modulus is due to an increase in mixing of repulsive A and B monomers. Under extension, this increase originates from a widening of the interface, and more molecules pulled free of the interface. Under compression, only the second of these two processes acts to increase the modulus. © 2004 American Institute of Physics. [DOI: 10.1063/1.1643899]

I. INTRODUCTION

Deducing the macroscopic mechanical properties of a material from a knowledge of the microscopic structure is a standard objective of material science.¹ While this objective has been largely realized in some subfields of material science, the theoretical study of block copolymer structure–property relationships is somewhat less developed. This is a serious gap in knowledge, given the rich variety of structures possible through the nanoscale self-assembly of block copolymers. Efforts have been made to understand the elastic properties of diblock copolymers in the lamellar phase using a variety of methods.^{2,3} Progress has also been made by Tyler and Morse⁴ using a method proposed by Kossuth, Morse, and Bates⁵ for obtaining the linear elastic properties of the cubic phases of diblock copolymers. They study the gyroid and body-centered-cubic phases of diblocks using standard linear elasticity theory⁶ and self-consistent field theory (SCFT).⁷

Studies of diblock copolymers alone avoids an important feature affecting the mechanical properties of block copolymers. The ability of intermediate blocks of *multiblock* copolymers to bridge between different chemical domains means that pseudo-“cross links” can form, which may be expected to have a profound effect on the elastic moduli.^{8,9} SCFT calculations have shown that the fraction of blocks that bridge between domains increases as a function of the number of blocks in a multiblock.¹⁰ Experimentally, increases in the elastic moduli as a function of block number have also been found in multiblock systems.¹¹ It is natural to assume that the increased bridging, or “cross linking,” is responsible for the increase in moduli.

In this article, we demonstrate that this is *not* the case. Using the approach of Tyler and Morse,⁴ a real space method for calculating the elastic moduli for block copolymers is presented. We apply our real space method to find the linear

elastic response of the lamellar phase of multiblock copolymer melts. Attention is limited to AB symmetric diblock copolymers tethered together to form multiblocks. Also, we consider only the melt state so that SCFT is applicable. Small distortions where linear elasticity theory can be applied are examined, and only quasi-equilibrium distortions are applied. If melt samples are distorted too quickly, the material will be in a nonequilibrium state, and the SCFT method would be inappropriate (typical SCFT is a theory for equilibrium and metastable states only). On the other hand, if samples are distorted too slowly, they will undergo nonlocal monomer redistribution, reaching the equilibrium period size. Thus, we would find zero moduli for all deformations. The intermediate time regime where we have quasi-equilibrium structures is actually quite large, and corresponds to many realistic situations.³ We, therefore, apply the current approach with expectations of at least qualitative agreement with experiments.

Qualitative agreement is found with the experimental results of Spontak and Smith¹¹ for the increase of tensile modulus of multiblock copolymers with increasing block numbers. Such increases in moduli are usually associated with an increase in the bridging fraction of intermediate blocks.^{8–11} Although there exists a corresponding increase of bridging fraction in multiblock copolymers with block number,¹⁰ our results indicate that it is *not* the cause of the increase in tensile modulus. Rather, the increase of modulus with block number is shown to be due to an increase of mixing between repulsive A and B monomers upon deformation. Under extension, this increase is due to a widening of the interface with more molecules pulled free of the interface. This means there will be more monomers of the “incorrect” type present in the bulk regions (away from the interfaces) of the lamellar structures. In compression, there is no significant change in the interfacial width. However, there is an increase of A/B monomers in the B/A regions.

^{a)}Electronic mail: rthompson@lanl.gov

^{b)}Author to whom correspondence should be addressed.

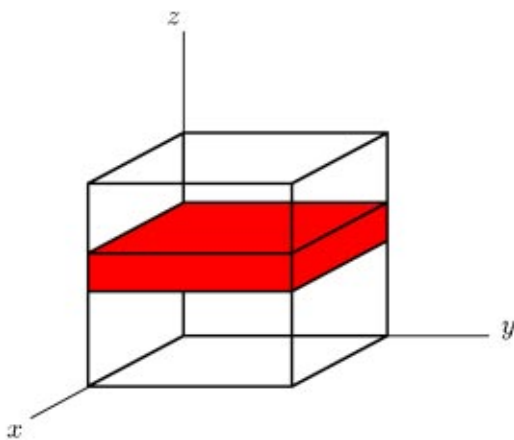


FIG. 1. Schematic of a lamellar material. The shaded band shows a lamellar stripe. Extensions in either the x or y directions will not change the periodicity of the structure, and therefore should have no effect on the free energy.

II. THEORY

We use the standard theory of linear elasticity⁶ and write the elastic free energy as

$$F_{el} = \frac{1}{2} K_{ijkl} u_{ij} u_{kl}, \quad (1)$$

where summation over repeated indices is implied. In Eq. (1), the strain tensor u_{ij} is given by

$$u_{ij} = \frac{1}{2} \left(\frac{\partial u_i}{\partial x_j} + \frac{\partial u_j}{\partial x_i} \right), \quad (2)$$

where u_i are the components of the displacement vector. From Eq. (1), the components of the elastic modulus tensor can be calculated as

$$K_{ijkl} = \left. \frac{\partial^2 F}{\partial u_{ij} \partial u_{kl}} \right|_{\mathbf{u}=0}, \quad (3)$$

where $\mathbf{u}=0$ denotes a strain tensor with zero components. We are particularly interested in lamellar materials with one preferred axis. For tetragonal symmetry with a preferred z axis, Eq. (1) simplifies to

$$F_{el} = \frac{1}{2} [K_{11}(u_{xx}^2 + u_{yy}^2) + 2K_{12}u_{xx}u_{yy} + 2(K_{11} - K_{12})u_{xz}^2 + K_{33}u_{zz}^2 + 4K_{44}(u_{yz}^2 + u_{xz}^2) + 2K_{13}(u_{xx} + u_{yy})u_{zz}], \quad (4)$$

where K_{lm} are the elastic constants in the Voigt notation. As pointed out by Tyler and Morse, the moduli of interest are measures of the “change in free energy caused by an isotropic change in the crystal domain spacing at constant polymer density, and not the (moduli) of the polymer melt, which is treated as incompressible.”⁴ As such, it is clear that an extension along either the x or y directions (directions in the xy plane parallel to the lamellae, see Fig. 1) would have no effect on the free energy. Therefore, the elastic free energy for a lamellar block copolymer reduces to

$$F_{el} = \frac{1}{2} [K_{33}u_{zz}^2 + 4K_{44}(u_{yz}^2 + u_{xz}^2)], \quad (5)$$

where K_{33} and K_{44} are the extensional and shear moduli, respectively. These may be calculated by distorting the material in the relevant directions. By stretching the material

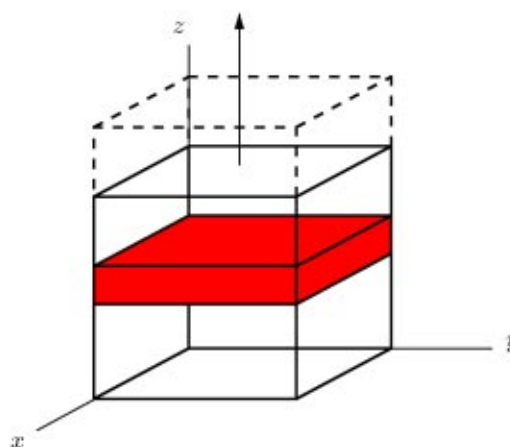


FIG. 2. Schematic of the material undergoing an extension along the z axis. Each side of the cube has length l before deformation (solid lines), but the z dimension of the object has a length $l + \epsilon$ after deformation (dashed lines). The shaded lamellar stripe is shown only before the distortion. The amount of deformation has been exaggerated.

along the z axis as shown in Fig. 2, we preserve neither volume nor shape. However, in this case only the u_{zz} component of the strain tensor is nonzero; it will have a value of ϵ/l , where ϵ is the absolute extension, and l is the length of the material in the z direction before extension. Equation (5) for the elastic free energy reduces to $F_{el} = \frac{1}{2} K_{33} \epsilon^2$, where ϵ is the relative extension, ϵ/l , and K_{33} is obtained from the second derivative. The modulus K_{44} is obtained by shearing the object along a plane perpendicular to the y axis, as shown in Fig. 3. The cubic object becomes a parallelepiped, with the xz face at $y=l$ shifted by an amount ϵ in the $+z$ direction, while the face at $y=0$ remains stationary. The only nonzero strain tensor component for such a deformation is $u_{yz} = \epsilon/2l$. Thus, the second derivative of the lamellar elastic free energy (5) yields K_{44} .

The free energy for a multiblock copolymer melt can be written in the context of SCFT as¹⁰

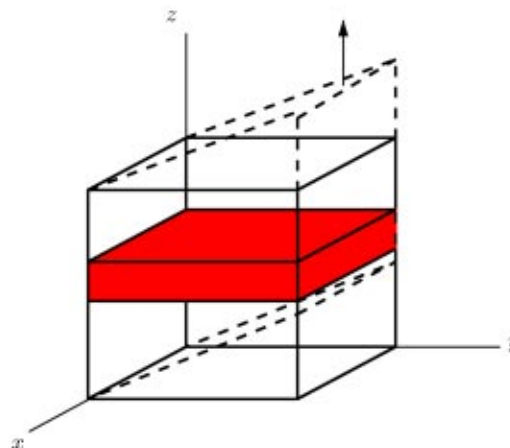


FIG. 3. Schematic of a material undergoing a shear. The cubic shape is distorted into a parallelepiped. Each side of the cube has length l before deformation (solid lines), as does each side of the parallelepiped after deformation (dashed lines). The shaded lamellar stripe is shown only before the distortion. The amount of deformation has been exaggerated.

$$\begin{aligned} \frac{F}{nk_B T} = & -\ln\left(\frac{Q}{V}\right) + \frac{1}{V} \int d\mathbf{r} \{ \chi N \varphi_A(\mathbf{r}) \varphi_B(\mathbf{r}) \\ & - w_A(\mathbf{r}) \varphi_A(\mathbf{r}) - w_B(\mathbf{r}) \varphi_B(\mathbf{r}) \\ & - \xi(\mathbf{r}) [1 - \varphi_A(\mathbf{r}) - \varphi_B(\mathbf{r})] \}, \end{aligned} \quad (6)$$

where $\varphi_A(\mathbf{r})$ and $\varphi_B(\mathbf{r})$ are the local volume fractions of *A* and *B* segments, respectively, $w_A(\mathbf{r})$ and $w_B(\mathbf{r})$ are the conjugate fields, and $\xi(\mathbf{r})$ is a pressure field enforcing incompressibility. The parameters χ and N refer to the segregation in a Flory–Huggins context, and the total number of segments in a multiblock, respectively, while k_B and T are Boltzmann's constant and temperature, respectively. V is the volume of the system and n is the number of molecules in the volume V . More details on SCFT can be found elsewhere.⁷ For this article, we assume a multiblock that is symmetric $(AB)_n$ so that *A* and *B* have the same volume fractions and $\chi N = 20n$. The statistical segment lengths a_A and a_B are assumed to be equal. Details of the numerics can be found in Refs. 12 and 13. In order to determine the elastic moduli K_{33} and K_{44} , we need to know the second derivative of the free energy with respect to the appropriate deformation ϵ . We can use Eq. (6) to numerically calculate the equilibrium free energy of a multiblock melt, as described in Refs. 12, 13. One can also calculate the free energy as a function of distortion ϵ by varying the size and shape of the SCFT calculation box according to Figs. 2 and 3. In principle, the system in the calculation box would rearrange itself so as to relieve the strain and revert to the equilibrium free energy for any distortion. However, we are using the numerical algorithm first introduced by Drolet and Fredrickson^{8,14} which searches for either equilibrium or metastable states. Thus, if the deformations are not too large, then the nearest numerical solution will, in fact, be the metastable strained state, and we can construct free energy versus ϵ curves. These curves may be verified to be parabolic for small deformations, and the curvature at $\epsilon=0$ would give the elastic moduli.

Specifically, extensions (Fig. 2) can be examined by computing the free energy of the lamellar system in the equilibrium box size, and then extending the box in a direction perpendicular to the lamellae by small increments ϵ , and recalculating the free energy at each increment. To examine shear is somewhat more involved. Again, we compute the equilibrium free energy in the natural box size, and then we shear the box by small increments as depicted in Fig. 3. The problem is that our numerical implementation assumes our evaluation points are arranged on a regular rectilinear grid, as shown in Fig. 4(a). In order to shear this sample, we must have a more general nonorthogonal spacing between evaluation points, as in Fig. 4(b). We can most easily accomplish this if we work in a nonorthogonal coordinate system. Then, the evaluation is the same except for places in the computation where nonlocal operations are performed, such as integrations or differentiations. In fact, after simplification, only one change needs to be made to the computation. Let us consider the coordinate transformation

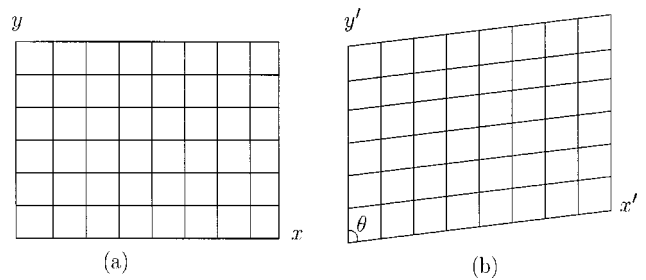


FIG. 4. (a) A rectilinear grid of evaluation points for numerical SCFT. For simplicity, only two dimensions are shown. (b) A more general nonorthogonal grid which results after a shear. The angle θ gives the amount of shear; if it is taken to be 90° , then we recover the rectangular grid. The amount of deformation has been exaggerated.

$$\begin{aligned} x' &= x, \\ y' &= \frac{y}{\sin \theta}, \\ z' &= z - y \cot \theta, \end{aligned} \quad (7)$$

where the primed coordinates are the nonorthogonal coordinates, the unprimed coordinates are the rectilinear coordinates, and θ is the angle describing the degree to which we are shearing our system. Thus, $\epsilon = \cot \theta$. For $\theta = \pi/2$, we regain a rectilinear system. To use such a nonorthogonal coordinate system, all integrals must be subjected to a change of variables, for which we will find a Jacobian determinant of $\sin \theta$. However, from the SCFT free energy (6), and the resulting mean field equations,¹⁰ the reader may verify that everywhere an integral appears, it is normalized by a volume. This volume must also be subjected to a factor $\sin \theta$, meaning that in the numerical implementation, no changes are required to use the nonorthogonal coordinate system, at least as far as integrals are concerned. Indeed, the only change that needs to be made is the use of a nonorthogonal Laplacian in the diffusion equation. (The diffusion equation has not been explicitly presented in this work, but is central to SCFT, see for example Matsen's review.⁷) Under the transformation (7), the Laplacian becomes

$$\begin{aligned} \nabla^2 &= \frac{\partial^2}{\partial x^2} + \frac{\partial^2}{\partial y^2} + \frac{\partial^2}{\partial z^2} \\ &= \frac{\partial^2}{\partial x'^2} + \frac{1}{\sin^2 \theta} \left(\frac{\partial^2}{\partial y'^2} + \frac{\partial^2}{\partial z'^2} - 2 \cos \theta \frac{\partial}{\partial y'} \frac{\partial}{\partial z'} \right) \\ &\equiv \nabla'^2. \end{aligned} \quad (8)$$

We are using an improved version of the algorithm of Drolet and Fredrickson^{8,14} based on the Fourier transform between real space and reciprocal space.^{12,13} Writing the Laplacian (8) in reciprocal space, where it is solved gives

$$\nabla'^2 = -k_x'^2 - \frac{1}{\sin^2 \theta} (k_y'^2 + k_z'^2 - 2k_y' k_z' \cos \theta). \quad (9)$$

It can be proven by substitution that the \mathbf{k}' wave vector is the wave vector that results from the application of a standard Fourier transform. In summary, if we perform a standard Fourier transform, use the Laplacian for our sheared system

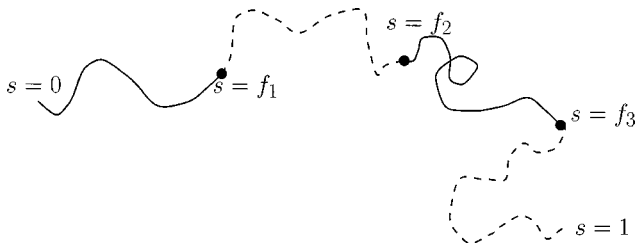


FIG. 5. Schematic of a multiblock copolymer $(A_n B_n)_p$, in this case, two joined diblocks, thus $p=2$. The A blocks are shown as solid curves, and the B blocks as dashed curves. The copolymer is parametrized along its length to run from $s=0$ to $s=1$, with the junction points labeled as f_i and marked with black dots. Thus, $f_0=0$ and $f_{2p}=1$.

as given by Eq. (9), and perform a standard inverse Fourier transform, then we will be calculating the diffusion equation for a nonorthogonal coordinate system, that is, a sheared system.

Our intention is to apply the above method to compare the elastic moduli for lamellae consisting of different order multiblock copolymers. This will provide insight into the effects of the increased block number on the mechanical properties. It will not tell us the physical origin of the effects. For this, we can analyze the *components* of the free energy as was originally suggested by Matsen and Bates.¹⁵ The free energy for a multiblock copolymer as depicted in Fig. 5 can be written as

$$\frac{F}{nk_B T} = \frac{U}{nk_B T} - T \left(\frac{S_E}{nk_B T} + \frac{S_C}{nk_B T} \right). \quad (10)$$

In Eq. (10), the entropy of the endpoint of a molecule ($s=1$) is denoted by S_E , whereas the conformational entropy of a molecule is given by S_C . The internal energy of the melt is given by U .

Let us consider only multiblocks comprised of tethered diblocks as shown in Fig. 5. The number of diblocks tethered together will denote the order p of our multiblock. The components of the free energy of such a system can be written as

$$\frac{U}{nk_B T} = \frac{\chi N}{V} \int d\mathbf{r} \varphi_A(\mathbf{r}) \varphi_B(\mathbf{r}), \quad (11)$$

$$\frac{-S_E}{nk_B} = \frac{1}{V} \int d\mathbf{r} \rho_E(\mathbf{r}) \ln \rho_E(\mathbf{r}), \quad (12)$$

$$\begin{aligned} \frac{-S_C}{nk_B} = & -\frac{1}{V} \int d\mathbf{r} [\rho_E(\mathbf{r}) \ln q(\mathbf{r}, 1) + w_A(\mathbf{r}) \varphi_A(\mathbf{r}) \\ & + w_B(\mathbf{r}) \varphi_B(\mathbf{r})], \end{aligned} \quad (13)$$

where

$$\rho_E(\mathbf{r}) = \frac{V}{Q} q(\mathbf{r}, 1). \quad (14)$$

Alternatively, one may think in terms of the components of the moduli K_{33} and K_{44} . Equation (10) may be twice differentiated to give

$$\frac{\partial^2 \left(\frac{F}{nk_B T} \right)}{\partial \epsilon^2} = \frac{\partial^2 \left(\frac{U}{nk_B T} \right)}{\partial \epsilon^2} + \frac{\partial^2 \left(\frac{-S_E}{nk_B} \right)}{\partial \epsilon^2} + \frac{\partial^2 \left(\frac{-S_C}{nk_B} \right)}{\partial \epsilon^2}. \quad (15)$$

This allows us to write

$$K_{33}^{\text{tot}} = K_{33}^U + K_{33}^{S_E} + K_{33}^{S_C}, \quad (16)$$

where the components K_{33}^U , $K_{33}^{S_E}$, and $K_{33}^{S_C}$ are identified with the derivatives in Eq. (15). A similar decomposition can be carried out for the modulus K_{44} .

In addition to observing and explaining multiblock copolymer elastic behavior from a purely theoretical point of view, it is useful to compare the theoretical results to experiment. The calculated elastic moduli K_{33} and K_{44} are not quantities that will be directly measured by experiments. They are for lamellar structures pertaining to a single crystal. Actual macroscopic specimens will likely be polycrystalline substances, with many lamellar domains oriented in random directions. This makes the sample a “quasi-isotropic” material, in that on macroscopic length scales, we expect it to have elastic properties that are the same in every direction. By taking the average over orientations of the lamellar domains according to the Voigt and Reuss averaging schemes, and in turn averaging these according to the prescription of Hill,¹⁶ the bulk modulus and shear modulus for the quasi-isotropic sample are found to be

$$B = \frac{K_{33}}{18}, \quad (17)$$

$$G = \frac{1}{30} (K_{33} + 6K_{44}). \quad (18)$$

We are not aware of experiments on multiblock copolymers that measure these two moduli as a function of diblock number. However, Spontak and Smith¹¹ have measured the tensile modulus of multiblock copolymers as a function of diblock number. Using a standard definition of the tensile (Young’s) modulus, E , in terms of the bulk and shear moduli,⁶ we find

$$E = \frac{K_{33}(K_{33} + 6K_{44})}{12(K_{33} + K_{44})}. \quad (19)$$

Expression (19) can be directly compared with the experimental results of Spontak and Smith.¹¹

III. RESULTS AND DISCUSSION

In order to compute the tensile modulus (19), we first need to calculate K_{33} and K_{44} for various multiblock copolymers. Figure 6 shows the free energy of a tetrablock copolymer ($p=2$) as a function of relative extension ϵ for both a regular extension (black dots) and a shear (black diamonds). As expected, these have parabolic shapes for small distortions. We therefore fit them with parabolas, and calculate the elastic moduli K_{33} and K_{44} . The results for different diblock numbers p are shown in Fig. 7. We note that the variation in the shear modulus K_{44} is much less significant than K_{33} . It should also be noted that there exists a large error on the K_{33}

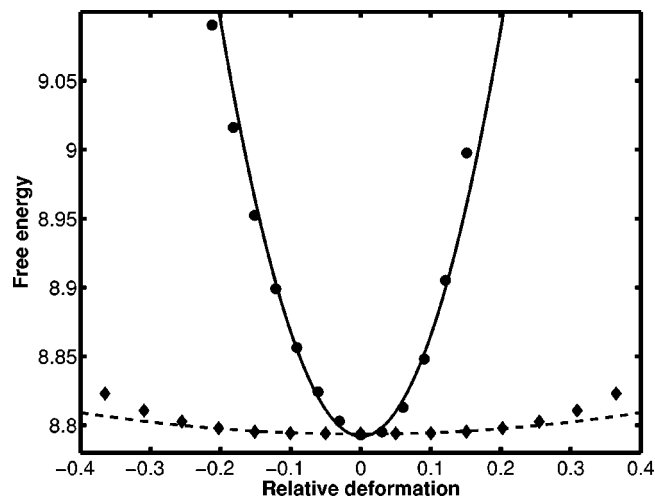


FIG. 6. Plot of free energy vs relative distortion ϵ for a tetrablock ($p=2$) copolymer. The points are the values calculated from SCFT with the black dots denoting an extension and the black diamonds indicating shear. The curves are parabolic fits to the data with the solid line fitting the extension data and the dashed line, the shear. For the extension data, negative values of deformation denote compressions whereas positive values denote extensions. All units are dimensionless.

and K_{44} values due to numerical accuracy limitations of the SCFT implementation and the arbitrariness of the parabolic fit. Since the linear elasticity theory is valid only for small extensions, the first few data points around equilibrium in Fig. 6 are the most important. Thus, only the first few points should be included in the fit. The cutoff is arbitrary though, and can affect the value of the moduli. This is particularly significant for the K_{44} modulus, which increases in value quickly with additional data points. The parabolic fit becomes poor however, so we omit the additional points, and find a small value of K_{44} with respect to K_{33} . Indeed, K_{44} is sufficiently small that it can be ignored in calculations of the tensile modulus E . The lack of variation of K_{44} is perhaps not altogether surprising, given that a number of polymer properties, such as in viscoelastic phase separation, are in-

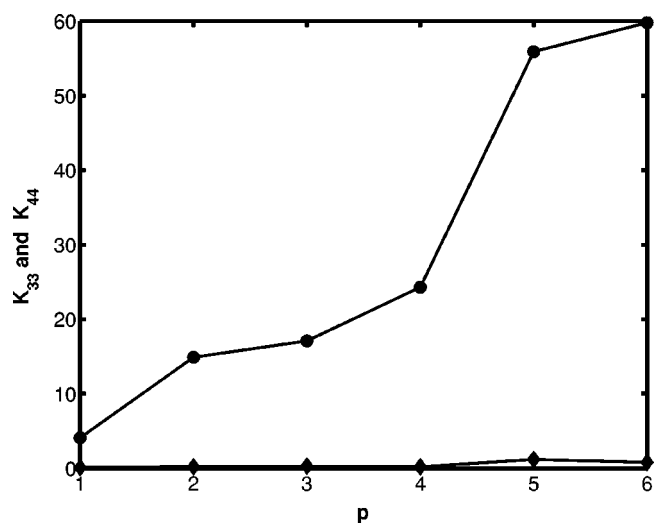


FIG. 7. Plot of the dimensionless elastic moduli vs diblock number p . K_{33} is denoted by black dots and K_{44} by black diamonds. The solid lines are guides for the eye.

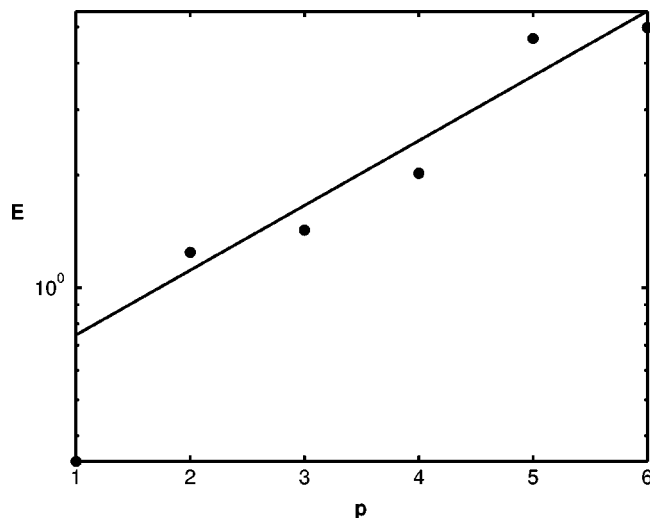


FIG. 8. Plot of the dimensionless tensile (Young's) modulus vs diblock number p . The black dots are the data points while the solid line is an exponential regression. The data is plotted on a semilog scale.

sensitive to changes in K_{44} .^{17,18} Neglecting K_{44} in Eq. (19) gives a tensile modulus that is directly proportional to K_{33} . A plot of E versus the diblock number p is shown in Fig. 8. Figure 8 shows that the tensile modulus increases with diblock number p , which is qualitatively consistent with experiment.¹¹ We have chosen to plot the data on a semilog scale, and so the line is an exponential fit.

With the qualitative agreement with experiment in mind, we can analyze the source of the increase of modulus with diblock number p . Table I gives the modulus K_{33} and its components as a function of p , according to Eq. (16). According to the bridging hypothesis for the strengthening of multiblock copolymers, the conformational entropy contribution to the free energy of the system should increase as the bridging blocks stretch,^{8–10} and so we should have a positive curvature. In Table I, the reverse is seen. For multiblocks, the total configurational entropy contribution seems to want to *help* in contracting or extending the substance. Table I shows that it is the *internal energy* that severely increases the curvature enough to cause the increase in the modulus despite the conformational entropy. This surprising result can be examined further. The free energy plot of Fig. 6 can be decomposed as shown in Fig. 9. The panel in Fig. 9(a) is the internal energy given by Eq. (11), and the panel in Fig. 9(b) is the sum of Eqs. (12) and (13), and gives the total entropy con-

TABLE I. Various components of the K_{33} modulus for different diblock numbers p . K_{33}^{tot} is the total modulus, and is the sum of K_{33}^U , K_{33}^{SE} , and K_{33}^{SC} , the internal energy, translational entropy, and configurational entropy contributions to the modulus, respectively.

p	K_{33}^{tot}	K_{33}^U	K_{33}^{SE}	K_{33}^{SC}
1	4.1	3.52	-0.58	1.18
2	14.9	38.32	-1.94	-21.47
3	17.1	46.47	-1.12	-28.25
4	24.3	71.36	-1.38	-45.73
5	55.9	110.36	-2.57	-51.92
6	59.8	119.26	-2.16	-57.33

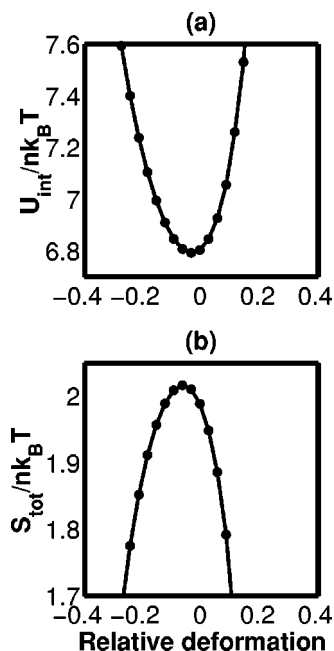


FIG. 9. Plot of the internal energy (a) and the total entropy (b) contributions to the free energy for a tetrablock copolymer. The data points are shown as black dots and the solid lines are guides for the eye. All units are dimensionless.

tribution to the free energy of the system. The example in Fig. 9 is for a tetrablock ($p=2$) copolymer. It again shows that the internal energy is solely responsible for the increase in energy around the equilibrium, and that the entropy contribution is actually near a local maximum. Thus, it appears that although the bridging fraction and modulus both increase with p ,^{10,11} the increased bridging fraction *does not cause* the increase in modulus, at least for quasi-equilibrium melt distortions in the linear regime, such as are studied here. This is perhaps not as surprising as it may seem. Matsen has pointed out the similarity between the equilibrium phase diagrams of AB diblocks and homologous ABA triblocks.⁹ For the latter system, he suggests that the bridging B blocks are quite relaxed *away* from the AB interfaces. Thus, upon “snipping” the triblocks to create diblocks, the system changes little, since the bridges are not “under tension.” A similar situation can be assumed to occur here in multiblock systems, such that small distortions close to equilibrium would have little impact on the elastic modulus, again since the bridges would not be under tension. Rather, the increase in modulus is caused by the internal energy, that is, an increase in mixing of A and B monomers upon distortion of the sample.

The mixing of A and B monomers upon distortion can be understood by examining Fig. 10, where we present a slice of the three-dimensional SCFT calculations for the density profiles of a tetrablock ($p=2$) system. The B segment profile for the system undergoing a tension is shown by the dotted-dashed curve. The equilibrium configuration for this system is shown by the solid curve. One can see that the interfacial width is greater for the extended structure than for the equilibrium one. Also, the density of monomers away from the interface is lower for the extended sample than for

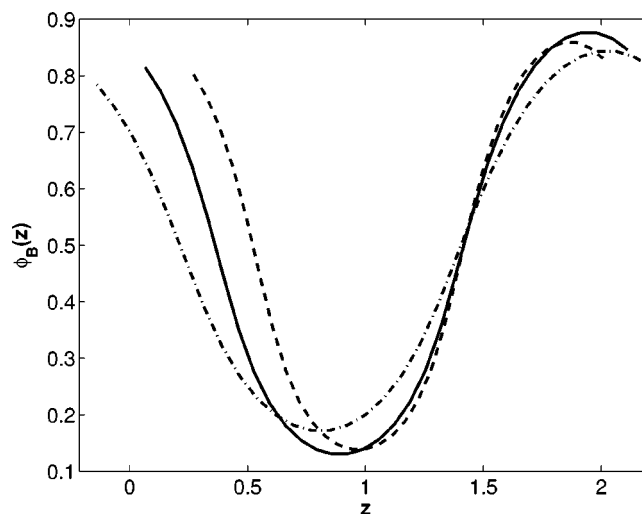


FIG. 10. Plot of the dimensionless B segment densities of a tetrablock copolymer ($p=2$) as a function of position. The black line shows the equilibrium configuration, the dashed line shows the system undergoing a compression, and the dotted-dashed line shows the results of an extension. The profiles are shifted so that the right-hand side most interface of each overlap. The z axis is in units of R_g , the radius of gyration of the polymer.

the equilibrium sample. Both of these features mean there are more AB contacts in the stretched system than the equilibrium system. The second feature corresponds to an increase of segments of the wrong type in each of the A/B domains. In other words, more molecules are free of the interfaces and are located within the bulk areas. The dashed line shows the B segment profile for a compressed system. The interfacial width is slightly narrower in this case, meaning there are fewer AB contacts. The density of monomers away from the interface is lower however, just as in the extended case. This will more than compensate for the narrower interfacial width, giving an overall increase in AB contacts, and thus in internal energy.

IV. CONCLUSIONS

We have studied the linear elastic properties of multiblock copolymer melts with molecules composed of tethered symmetric AB diblock copolymers. We have found a qualitative agreement with the experimental results of Spontak and Smith¹¹ for an increase in tensile modulus as a function of diblock number p . We have demonstrated that the conformational entropy contribution to the free energy does not increase with p , and thus discount the increase in bridging fraction¹⁰ as the cause for the increase in tensile modulus. We demonstrate instead that an increase in internal energy as a function of p is the cause of the increased modulus. The increased mixing of A and B segments which is responsible for the increase in internal energy is shown to be due to a greater number of molecules being pulled out of the interface to populate the “bulk” regions of the lamellar structure. This mechanism is present for both compressions and extensions. For extensions, a widening of the interface also plays a role.

ACKNOWLEDGMENT

Work at the Los Alamos National Laboratory was performed under the auspices (Contract No. W-7405-ENG-36) of the U.S. Department of Energy.

¹D. R. Askeland, *The Science and Engineering of Materials* (PWS-Kent, 1984).

²C. Yeung, A. C. Shi, J. Noolandi and R. C. Desai, *Macromol. Theory Simul.* **5**, 291 (1996), and references therein.

³Z. G. Wang, *J. Chem. Phys.* **100**, 2298 (1994).

⁴C. A. Tyler and D. C. Morse, *Macromolecules* **36**, 3764 (2003).

⁵M. B. Kossuth, D. C. Morse, and F. S. Bates, *J. Rheology* **43**, 167 (1999).

⁶L. D. Landau and E. M. Lifshitz, *Theory of Elasticity*, 3rd ed. (Butterworth-Heinemann, Oxford, 1999).

⁷M. W. Matsen, *J. Phys.: Condens. Matter* **14**, R21 (2002), and references therein.

⁸F. Drolet and G. H. Fredrickson, *Macromolecules* **34**, 5317 (2001).

⁹M. W. Matsen and R. B. Thompson, *J. Chem. Phys.* **111**, 7139 (1999).

¹⁰K. Ø. Rasmussen, E. M. Kober, T. Lookman, and A. Saxena, *J. Polym. Sci., Polym. Phys. Ed.* **41**, 104 (2003).

¹¹R. J. Spontak and S. D. Smith, *J. Polym. Sci., Polym. Phys. Ed.* **39**, 947 (2001).

¹²G. Tzeremes, K. Ø. Rasmussen, T. Lookman, and A. Saxena, *Phys. Rev. E* **65**, 041806 (2002).

¹³K. Ø. Rasmussen and G. Kalosakos, *J. Polym. Sci., Polym. Phys. Ed.* **40**, 1777 (2002).

¹⁴F. Drolet and G. H. Fredrickson, *Phys. Rev. Lett.* **83**, 4317 (1999).

¹⁵M. W. Matsen and F. S. Bates, *J. Chem. Phys.* **106**, 2436 (1997).

¹⁶E. Schreiber, O. L. Anderson, and N. Soga, *Elastic Constants and Their Measurement* (McGraw-Hill, Toronto, 1973).

¹⁷H. Tanaka, *J. Phys.: Condens. Matter* **12**, R207 (2000).

¹⁸Y. Huo, H. Zhang, and Y. Yang, *Macromolecules* **36**, 5383 (2003).